and 10 $Na_3HP_2O_7$. FV solution also contained 0.2 NaF and 0.1 Na_3VO_4. Rarely, irreversible current rundown still occurred with FVPP. The total Na^+ concentration of all cytoplasmic solutions was adjusted to 30 mM with NaOH, and pH was adjusted to 7.0 with *N*-methylglucamine (NMG) or HCl. PIP_2 liposomes (20–200 nm) were prepared by sonicating 1 mM PIP_2 (Boehringer Mannheim) in distilled water. Reconstituted monoclonal PIP_2 antibody (Perspective Biosystems, Framingham, MA) was diluted 40-fold into experimental solution. Current–voltage relations of all currents reversed at E_K and showed characteristic rectification, mostly owing to the presence of Na^+ in FVPP and possibly also residual polyamines. Current records presented (measured at 30 °C, −30 mV holding potential) are digitized strip-chart recordings. Purified bovine brain $G\beta\gamma$[29] was diluted just before application such that the final detergent (CHAPS) concentration was 5 μM. Detergent-containing solution was washed away thoroughly before application of PIP_2, because application of phospholipid vesicles in the presence of detergent usually reversed the effects of $G\beta\gamma$; presumably, $G\beta\gamma$ can be extracted from membranes by detergent plus phospholipids.

Molecular biology. R188Q mutation was constructed by insertion of the mutant oligonucleotides between the *Bsm*1 and *Bgl*II sites of pSPORT–ROMK1 (ref. 11). A polymerase chain reaction (PCR) fragment (amino acids 180–391) from pSPORT–ROMK1 R188Q mutant was subcloned into pGEX-2T vector (Pharmacia) for expression of R188Q mutant protein of GST–RKC. The construction, expression and purification of GST–IKC (amino acids 182–428 of IRK1), GST–GKC (180–462 of GIRK1), GST–IKN (1–86 of IRK1) have been described[21,22].

***In vitro* PIP_2 binding assay.** ^{3}H-PIP_2 in chloroform-methanol (1:1) (American Radiolabeled Chemicals; 0.4 μCi nM^{-1} specific activity) was dried under N_2 and sonicated in 100 μl phosphate buffered saline (PBS) to form pure ^{3}H-PIP_2 liposomes. Purified GST fusion protein (100 nM) was incubated with ^{3}H-PIP_2 (0.2–1 μM) and precipitated by glutathione 4B-Sepharose beads. After 1 wash with PBS, the precipitates were dissolved in SDS gel loading buffer and counted in a beta-scintillation counter using a window for ^{3}H. The bound ^{3}H radioactivity was typically in the range ~2–8% of the total added. For co-immunoprecipitation, 25% PIP_2 or PIP in 75% phosphatidylcholine (PC) background (30 μg PIP_2 or PIP (Boehringer Mannheim) and 90 μg phosphatidylcholine (Sigma)), both in chloroform, were dried down together and sonicated in 300 μl PBS to form mixed liposome. GST fusion proteins were first incubated with 25% PIP_2 or PIP liposome (100 μM) and PIP_2 antibodies (1:100 dilution) for 2 h and with protein A–Sepharose for a further 30 min. After one wash with PBS, the immunoprecipitates were separated by 10% SDS–PAGE, probed with specific antibodies[21,22], and visualized by ECL (Amersham). Each experiment was performed at least twice with similar results. The relative amount of immunoreactivity in each lane was quantified by serial dilutions of sample[21].

Received 6 June; accepted 13 October 1997.

1. McNicholas, C. M., Wang, W., Ho, K., Hebert, S. C. & Giebisch, G. Regulation of ROMK1 K^+ channel activity involves phosphorylation processes. *Proc. Natl Acad. Sci. USA* **91,** 8077–8081 (1994).
2. Fakler, B., Brandle, U., Glowatzki, E., Zenner, H.-P. & Ruppersberg, J. P. Kir2.1 inward rectifier K^+ channels are regulated independently by protein kinases and ATP hydrolysis. *Neuron* **13,** 1413–1420 (1994).
3. Kubo, Y., Reuveny, E., Slesinger, P. A., Jan, Y. N. & Jan, L. Y. Primary structure and functional expression of a rat G-protein-coupled muscarinic potassium channel. *Nature* **364,** 802–806 (1993).
4. Dascal, N. *et al.* Atrial G protein-activated K^+ channel: expression cloning and molecular properties. *Proc. Natl Acad. Sci. USA* **90,** 10235–10239 (1993).
5. Krapivinsky, G. *et al.* The G-protein-gated atrial K^+ channel I_{KACh} is a heteromultimer of two inwardly rectifying K^+-channel proteins. *Nature* **374,** 135–141 (1995).
6. Lesage, F. *et al.* Molecular properties of neuronal G protein-activated inwardly rectifying K^+ channels. *J. Biol. Chem.* **270,** 28660–28667 (1995).
7. Furukawa, T., Yamane, T., Terai, T., Katayama, Y. & Hiraoka, M. Functional linkage of the cardiac ATP-sensitive K^+ channel to actin cytoskeleton. *Pflugers Arch.* **431,** 504–512 (1996).
8. Hilgemann, D. W. & Ball, R. Regulationof cardiac Na^+, Ca^{2+} exchange and K_{ATP} potassium channels by PIP_2. *Science* **273,** 956–959 (1996).
9. Fukami, K. *et al.* Antibody to phosphatidylinositol 4,5-bisphosphate inhibits oncogene-induced mitogenesis. *Proc. Natl Acad. Sci. USA* **85,** 9057–9061 (1988).
10. Kubo, Y., Baldwin, T. J., Jan, Y. N. & Jan, L. Y. Primary structure and functional expression of a mouse inward rectifier potassium channel. *Nature* **362,** 127–133 (1993).
11. Ho, K. *et al.* Cloning and expression of an inwardly rectifying ATP-regulated potassium channel. *Nature* **362,** 31–38 (1993).
12. Sui, J. L., Chan, K. W. & Logothetis, D. E. Na^+ activation of the muscarinic K^+ channel by a G-protein-independent mechanism. *J. Gen. Physiol.* **109,** 381–390 (1996).
13. Chan, K. W. *et al.* A recombinant inwardly rectifying potassium channel coupled to GTP-binding proteins. *J. Gen. Physiol.* **107,** 381–397 (1996).
14. Zhang, X., Jefferson, A. B., Auethavekiat, V. & Majerus, P. W. The protein deficient in Lowe syndrome is a phosphatidylinositol-4,5-bisphosphate 5-phosphatase. *Proc. Natl Acad. Sci. USA* **92,** 4853–4856 (1995).
15. Fukami, K., Endo, T., Imamura, M. & Takenawa, T. α-Actinin and vinculin are PIP_2-binding proteins involved in signaling by tyrosine kinase. *J. Biol. Chem.* **269,** 1518–1522 (1994).
16. Fan, Z. & Makielski, J. C. Anionic phospholipids activate ATP-sensitive potassium channels. *J. Biol. Chem.* **272,** 5388–5395 (1997).
17. Schacht, J. Inhibition by neomycin of polyphosphoinositide turnover in subcellular fractions of guinea-pig cerebral cortex *in vitro*. *J. Neurochem.* **27,** 1119–1124 (1976).
18. Kim, J., Mosior, M., Chung, L. A., Wu, H. & McLaughlin, S. Binding of peptides with basic residues to membrane containing acidic phospholipids. *Biophys. J.* **60,** 135–148 (1991).
19. Harlan, J. E., Yoon, H. S., Hajduk, P. J. & Fesik, S. W. Structural characterization of the interaction between a pleckstrin homology domain and phosphatidylinositol 4,5-bisphosphate. *Biochemistry* **34,** 9859–9864 (1995).
20. Reuveny, E. *et al.* Activation of the cloned muscarinic potassium channel by G protein $\beta\gamma$ subunits. *Nature* **370,** 143–146 (1994).
21. Huang, C.-L., Slesinger, P. A., Casey, P. J., Jan, Y. N. & Jan, L. Y. Evidence that direct binding of $G_{\beta\gamma}$ to the GIRK1 protein-gated inwardly rectifying K^+ channel is important for channel activation. *Neuron* **15,** 1133–1143 (1995).
22. Huang, C.-L., Jan, Y. N. & Jan, L. Y. Binding of $G_{\beta\gamma}$ to multiple regions of G protein-gated inward rectifier K^+ channels. *FEBS Lett.* **405,** 291–298 (1997).
23. Krapivinsky, G., Krapivinsky, L., Wickman, K. & Clapham, D. E. $G\beta\gamma$ binds directly to the G protein-gated K^+ channel, I_{KACh}. *J. Biol. Chem.* **270,** 29059–29062 (1995).
24. Janmey, P. A. Phosphoinositides and calcium as regulators of cellular actin assembly and disassembly. *Annu. Rev. Physiol.* **56,** 169–191 (1994).
25. Penniston, J. T. Plasma membrane Ca^{2+}-pumping ATPases. *Ann. NY Acad. Sci.* **402,** 291–303 (1982).
26. Pitcher, J. A., Touhara, K., Payne, E. S. & Lefkowitz, R. J. Pleckstrin homology domain-mediated membrane association and activation of the β-adrenergic receptor kinase requires coordinate interaction with $G\beta\gamma$ and lipid. *J. Biol. Chem.* **270,** 11707–11710 (1995).
27. Tagliaalatela, M., Wible, B. A., Caporaso, R. & Brown, A. M. Specification of the pore properties by the carboxyl terminus of inward rectifying K^+ channels. *Science* **264,** 844–847 (1994).
28. Clapham, D. E. & Neer, E. J. New roles for G protein $\beta\gamma$-dimers in transmembrane signaling. *Nature* **365,** 403–406 (1993).
29. Casey, P. J., Graziano, M. P. & Gilman, A. G. G protein $\beta\gamma$ subunits from bovine brain and retina: equivalent catalytic support of ADP-ribosylation of α subunit by pertussis toxin but differential interactions with G_{α}. *Biochemistry* **28,** 611–616 (1989).

Acknowledgements. We thank E. Phan for technical assistance; I. Bezprozvanny, C. Dessauer, D. Logothetis, C.-C. Lu, O. Moe, S. Muallem and H. Yin for discussions and advice; L. Jan for GIRK1 and ROMK1 antibodies; C. Dessauer and A. Gilman for $G\alpha_{i1}$; P. Casey for $G\beta\gamma$; and R. Alpern for support and encouragement. This work was supported by grants from the NKF of Texas (C.L.H.) and from the AHA and NIH (D.W.H.).

Correspondence and requests for materials should be addressed to C.L.H. (e-mail: chuan1@mednet.swmed.edu).

Potent and specific genetic interference by double-stranded RNA in *Caenorhabditis elegans*

Andrew Fire*, SiQun Xu*, Mary K. Montgomery*, Steven A. Kostas*†, Samuel E. Driver‡ & Craig C. Mello‡

** Carnegie Institution of Washington, Department of Embryology, 115 West University Parkway, Baltimore, Maryland 21210, USA*
† Biology Graduate Program, Johns Hopkins University, 3400 North Charles Street, Baltimore, Maryland 21218, USA
‡ Program in Molecular Medicine, Department of Cell Biology, University of Massachusetts Cancer Center, Two Biotech Suite 213, 373 Plantation Street, Worcester, Massachusetts 01605, USA

Experimental introduction of RNA into cells can be used in certain biological systems to interfere with the function of an endogenous gene[1,2]. Such effects have been proposed to result from a simple antisense mechanism that depends on hybridization between the injected RNA and endogenous messenger RNA transcripts. RNA interference has been used in the nematode *Caenorhabditis elegans* to manipulate gene expression[3,4]. Here we investigate the requirements for structure and delivery of the interfering RNA. To our surprise, we found that double-stranded RNA was substantially more effective at producing interference than was either strand individually. After injection into adult animals, purified single strands had at most a modest effect, whereas double-stranded mixtures caused potent and specific interference. The effects of this interference were evident in both the injected animals and their progeny. Only a few molecules of injected double-stranded RNA were required per affected cell, arguing against stochiometric interference with endogenous

mRNA and suggesting that there could be a catalytic or amplification component in the interference process.

Despite the usefulness of RNA interference in *C. elegans*, two features of the process have been difficult to explain. First, sense and antisense RNA preparations are each sufficient to cause interference[3,4]. Second, interference effects can persist well into the next generation, even though many endogenous RNA transcripts are rapidly degraded in the early embryo[5]. These results indicate a fundamental difference in behaviour between native RNAs (for example, mRNAs) and the molecules responsible for interference. We sought to test the possibility that this contrast reflects an underlying difference in RNA structure. RNA populations to be injected are generally prepared using bacteriophage RNA polymerases[6]. These polymerases, although highly specific, produce some random or ectopic transcripts. DNA transgene arrays also produce a fraction of aberrant RNA products[3]. From these facts, we surmised that the interfering RNA populations might include some molecules with double-stranded character. To test whether double-stranded character might contribute to interference, we further purified single-stranded RNAs and compared interference activities of individual strands with the activity of a deliberately prepared double-stranded hybrid.

The *unc-22* gene was chosen for initial comparisons of activity. *unc22* encodes an abundant but nonessential myofilament protein[7–9]. Several thousand copies of *unc-22* mRNA are present in each

Table 1 Effects of sense, antisense and mixed RNAs on progeny of injected animals

Gene	segment	Size (kilobases)	Injected RNA	F_1 phenotype
unc-22				*unc-22*-null mutants: strong twitchers[7,8]
*unc22A**	Exon 21–22	742	Sense	Wild type
			Antisense	Wild type
			Sense + antisense	Strong twitchers (100%)
unc22B	Exon 27	1,033	Sense	Wild type
			Antisense	Wild type
			Sense + antisense	Strong twitchers (100%)
unc22C	Exon 21–22†	785	Sense + antisense	Strong twitchers (100%)
fem-1				*fem-1*-null mutants: femal (no sperm)[13]
fem1A	Exon 10‡	531	Sense	Hermaphrodite (98%)
			Antisense	Hermaphrodite (>98%)
			Sense + antisense	Female (72%)
fem1B	Intron 8	556	Sense + antisense	Hermaphrodite (>98%)
unc-54				*unc-54*-null mutants: paralysed[7,11]
unc54A	Exon 6	576	Sense	Wild type (100%)
			Antisense	Wild type (100%)
			Sense + antisense	Paralysed (100%)§
unc54B	Exon 6	651	Sense	Wild type (100%)
			Antisense	Wild type (100%)
			Sense + antisense	Paralysed (100%)§
unc54C	Exon 1–5	1,015	Sense + antisense	Arrested embryos and larvae (100%)
unc54D	Promoter	567	Sense + antisense	Wild type (100%)
unc54E	Intron 1	369	Sense + antisense	Wild type (100%)
unc54F	Intron 3	386	Sense + antisense	Wild type (100%)
hlh-1				*hlh-1*-null mutants: lumpy-dumpy larvae[16]
hlh1A	Exons 1–6	1,033	Sense	Wild type (<2% lpy-dpy)
			Antisense	Wild type (<2% lpy-dpy)
			Sense + antisense	Lpy-dpy larvae (>90%)‖
hlh1B	Exons 1–2	438	Sense + antisense	Lpy-dpy larvae (>80%)‖
hlh1C	Exons 4–6	299	Sense + antisense	Lpy-dpy larvae (>80%)‖
hlh1D	Intron 1	697	Sense + antisense	Wild type (<2% lpy-dpy)
myo-3-driven GFP transgenes¶				
myo-3::NLS::gfp::lacZ				Makes nuclear GFP in body muscle
gfpG	Exons 2–5	730	Sense	Nuclear GFP–LacZ pattern of parent strain
			Antisense	Nuclear GFP–LacZ pattern of parent strain
			Sense + antisense	Nuclear GFP–LacZ absent in 98% of cells
lacZL	Exon 12–14	830	Sense + antisense	Nuclear GFP–LacZ absent in >95% of cells
myo-3::MtLS::gfp				Makes mitochondrial GFP in body muscle
gfpG	Exons 2–5	730	Sense	Mitochondrial-GFP pattern of parent strain
			Antisense	Mitochondrial-GFP pattern of parent strain
			Sense + antisense	Mitochondrial-GFP absent in 98% of cells
lacZL	Exon 12–14	830	Sense + antisense	Mitochondrial-GFP pattern of parent strain

Each RNA was injected into 6–10 adult hermaphrodites (0.5×10^6–1×10^6 molecules into each gonad arm). After 4–6 h (to clear prefertilized eggs from the uterus), injected animals were transferred and eggs collected for 20–22 h. Progeny phenotypes were scored upon hatching and subsequently at 12-24-h intervals.

* to obtain a semiquantitative assessment of the relationship between RNA dose and phenotypic response, we injected each *unc22A* RNA preparation at a series of different concentrations (see figure in Supplementary information for details). At the highest dose tested (3.6×10^6 molecules per gonad), the individual sense and antisense *unc22A* preparations produced some visible twitching (1% and 11% of progeny, respectively). Comparable doses of double-stranded *unc22A* RNA produced visible twitching in all progeny, whereas a 120-fold lower dose of double-stranded *unc22A* RNA produced visible twitching in 30% of progeny. † *unc22C* also carries the 43-nucleotide intron between exons 21 and 22. ‡ *fem1A* carries a portion (131 nucleotides) of intron 10. § Animals in the first affected broods (layed 4–24 h after injection) showed movement defects indistinguishable from those of *unc-54*-null mutants. A variable fraction of these animals (25%–75%) failed to lay eggs (another phenotype of *unc-54*-null mutants), whereas the remainder of the paralysed animals did lay eggs. This may indicate incomplete interference with *unc-54* activity in vulval muscles. Animals from later broods frequently show a distinct partial loss-of-function phenotype, with contractility in a subset of body-wall muscles. ‖ Phenotypes produced by RNA-mediated interference with *hlh-1* included arrested embryos and partially elongated L1 larvae (the *hlh-1*-null phenotype). These phenotypes were seen in virtually all progeny after injection of double-stranded *hlh1A* and in about half of the affected animals produced after injection of double-stranded *hlh1B* and double-stranded *hlh1C*. A set of less severe defects was seen in the remainder of the animals produced after injection of double-stranded *hlh1B* and double-stranded *hlh1C*). The less severe phenotypes are characteristic of partial loss of function of *hlh-1* (B. Harfe and A.F., unpublished observations). ¶ the host for these injections, strain PD4251, expresses both mitochondrial GFP and nuclear GFP–LacZ (see Methods). This allows simultaneous assay for interference with *gfp* (seen as loss of all fluorescence) and with *lacZ* (loss of nuclear fluorescence). The table describes scoring of animals as L1 larvae. Double-stranded *gfpG* caused a loss of GFP in all but 0–3 of the 85 body muscles in these larvae. As these animals mature to adults, GFP activity was seen in 0–5 additional body-wall muscles and in the 8 vulval muscles. Lpy-dpy, lumpy-dumpy.

striated muscle cell[3]. Semiquantitative correlations between *unc-22* activity and phenotype of the organism have been described[8]: decreases in *unc-22* activity produce an increasingly severe twitching phenotype, whereas complete loss of function results in the additional appearance of muscle structural defects and impaired motility.

Purified antisense and sense RNAs covering a 742-nucleotide segment of *unc-22* had only marginal interference activity, requiring a very high dose of injected RNA to produce any observable effect (Table 1). In contrast, a sense–antisense mixture produced highly effective interference with endogenous gene activity. The mixture was at least two orders of magnitude more effective than either single strand alone in producing genetic interference. The lowest dose of the sense–antisense mixture that was tested, ~60,000 molecules of each strand per adult, led to twitching phenotypes in an average of 100 progeny. Expression of *unc-22* begins in embryos containing ~500 cells. At this point, the original injected material would be diluted to at most a few molecules per cell.

The potent interfering activity of the sense–antisense mixture could reflect the formation of double-stranded RNA (dsRNA) or, conceivably, some other synergy between the strands. Electrophoretic analysis indicated that the injected material was predominantly double-stranded. The dsRNA was gel-purified from the annealed mixture and found to retain potent interfering activity. Although annealing before injection was compatible with interference, it was not necessary. Mixing of sense and antisense RNAs in low-salt concentrations (under conditions of minimal dsRNA formation) or rapid sequential injection of sense and antisense strands were sufficient to allow complete interference. A long interval (>1 h) between sequential injections of sense and antisense RNA resulted in a dramatic decrease in interfering activity. This suggests that injected single strands may be degraded or otherwise rendered inaccessible in the absence of the opposite strand.

A question of specificity arises when considering known cellular responses to dsRNA. Some organisms have a dsRNA-dependent protein kinase that activates a panic-response mechanism[10]. Conceivably, our sense–antisense synergy might have reflected a non-specific potentiation of antisense effects by such a panic mechanism. This is not the case: co-injection of dsRNA segments unrelated to *unc-22* did not potentiate the ability of single *unc-22*-RNA strands to mediate inhibition (data not shown). We also investigated whether double-stranded structure could potentiate interference activity when placed in *cis* to a single-stranded segment. No such potentiation was seen: unrelated double-stranded sequences located 5′ or 3′ of a single-stranded *unc-22* segment did not stimulate interference. Thus, we have only observed potentiation of interference when dsRNA sequences exist within the region of homology with the target gene.

The phenotype produced by interference using *unc-22* dsRNA was extremely specific. Progeny of injected animals exhibited behaviour that precisely mimics loss-of-function mutations in *unc-22*. We assessed target specificity of dsRNA effects using three additional genes with well characterized phenotypes (Fig. 1, Table 1). *unc-54* encodes a body-wall-muscle heavy-chain isoform of myosin that is required for full muscle contraction[7,11,12]; *fem-1* encodes an ankyrin-repeat-containing protein that is required in hermaphrodites for sperm production[13,14]; and *hlh-1* encodes a *C. elegans* homologue of myoD-family proteins that is required for proper body shape and motility[15,16]. For each of these genes, injection of related dsRNA produced progeny broods exhibiting

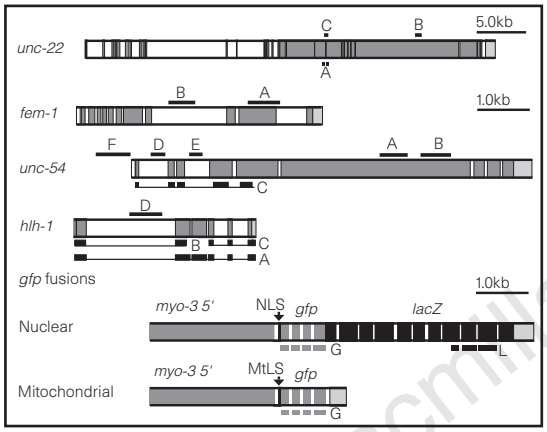

Figure 1 Genes used to study RNA-mediated genetic interference in *C. elegans*. Intron–exon structure for genes used to test RNA-mediated inhibition are shown (grey and filled boxes, exons; open boxes, introns; patterned and striped boxes, 5′ and 3′ untranslated regions. *unc-22*, ref. 9, *unc-54*, ref. 12, *fem-1*, ref. 14, and *hlh-1*, ref. 15). Each segment of a gene tested for RNA interference is designated with the name of the gene followed by a single letter (for example, *unc22C*). These segments are indicated by bars and upper-case letters above and below each gene. Segments derived from genomic DNA are shown above the gene; segments derived from cDNA are shown below the gene. NLS, nuclear-localization sequence; MtLS, mitochondrial localization sequence.

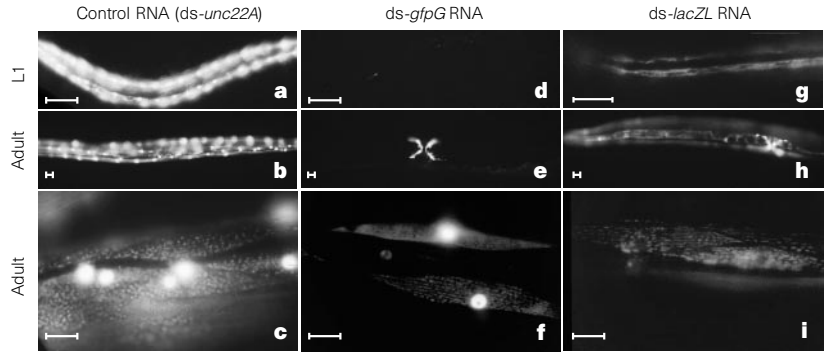

Figure 2 Analysis of RNA-interference effects in individual cells.Fluorescence micrographs show progeny of injected animals from GFP-reporter strain PD4251. **a**–**c**, Progeny of animals injected with a control RNA (double-stranded (ds)-*unc22A*). **a**, Young larva, **b**, adult, **c**, adult body wall at high magnification. These GFP patterns appear identical to patterns in the parent strain, with prominent fluorescence in nuclei (nuclear-localized GFP–LacZ) and mitochondria (mitochondrially targeted GFP). **d**–**f**, Progeny of animals injected with ds-*gfpG*. Only a single active cell is seen in the larva in **d**, whereas the entire vulval musculature expresses active GFP in the adult animal in **e**. **f**, Two rare GFP-positive cells in an adult: both cells express both nuclear-targeted GFP–LacZ and mitochondrial GFP. **g**–**i**, Progeny of animals injected with ds-*lacZL* RNA: mitochondrial-targeted GFP seems unaffected, while the nuclear-targeted GFP–LacZ is absent from almost all cells (for example, see larva in **g**). **h**, A typical adult, with nuclear GFP–LacZ lacking in almost all body-wall muscles but retained in vulval muscles. Scale bars represent 20 μm.

the known null-mutant phenotype, whereas the purified single RNA strands produced no significant interference. With one exception, all of the phenotypic consequences of dsRNA injection were those expected from interference with the corresponding gene. The exception (segment *unc54C* which led to an embryonic- and larval-arrest phenotype not seen with *unc-54*-null mutants) was illustrative. This segment covers the highly conserved myosin-motor domain, and might have been expected to interfere with activity of other highly related myosin heavy-chain genes[17]. The *unc54C* segment has been unique in our overall experience to date: effects of 18 other dsRNA segments (Table 1; and our unpublished observations) have all been limited to those expected from previously characterized null mutants.

The pronounced phenotypes seen following dsRNA injection indicate that interference effects are occurring in a high fraction of cells. The phenotypes seen in *unc-54* and *hlh-1* null mutants, in particular, are known to result from many defective muscle cells[11,16]. To examine interference effects of dsRNA at a cellular level, we used a transgenic line expressing two different green fluorescent protein (GFP)-derived fluorescent-reporter proteins in body muscle. Injection of dsRNA directed to *gfp* produced marked decreases in the fraction of fluorescent cells (Fig. 2). Both reporter proteins were absent from the affected cells, whereas the few cells that were fluorescent generally expressed both GFP proteins.

The mosaic pattern observed in the *gfp*-interference experiments was nonrandom. At low doses of dsRNA, we saw frequent interference in the embryonically derived muscle cells that are present when the animal hatches. The interference effect in these differentiated cells persisted throughout larval growth: these cells produced little or no additional GFP as the affected animals grew. The 14 postembryonically derived striated muscles are born during early larval stages and these were more resistant to interference. These cells have come through additional divisions (13–14 divisions versus 8–9 divisions for embryonic muscles[18,19]). At high concentrations of *gfp* dsRNA, we saw interference in virtually all striated body-wall muscles, with occasional lone escaping cells, including cells born during both embryonic and postembryonic development. The non-striated vulval muscles, which are born during late larval development, appeared to be resistant to interference at all tested concentrations of injected dsRNA.

We do not yet know the mechanism of RNA-mediated interference in *C. elegans*. Some observations, however, add to the debate about possible targets and mechanisms.

First, dsRNA segments corresponding to various intron and promoter sequences did not produce detectable interference (Table 1). Although consistent with interference at a post-transcriptional level, these experiments do not rule out interference at the level of the gene.

Second, we found that injection of dsRNA produces a pronounced decrease or elimination of the endogenous mRNA transcript (Fig. 3). For this experiment, we used a target transcript (*mex-3*) that is abundant in the gonad and early embryos[20], in which straightforward *in situ* hybridization can be performed[5]. No endogenous *mex-3* mRNA was observed in animals injected with a dsRNA segment derived from *mex-3*. In contrast, animals into which purified *mex-3* antisense RNA was injected retained substantial endogenous mRNA levels (Fig. 3d).

Third, dsRNA-mediated interference showed a surprising ability to cross cellular boundaries. Injection of dsRNA (for *unc-22*, *gfp* or *lacZ*) into the body cavity of the head or tail produced a specific and robust interference with gene expression in the progeny brood (Table 2). Interference was seen in the progeny of both gonad arms, ruling out the occurrence of a transient 'nicking' of the gonad

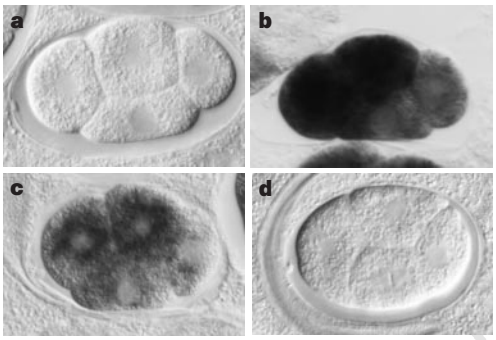

Figure 3 Effects of *mex-3* RNA interference on levels of the endogenous mRNA. Interference contrast micrographs show *in situ* hybridization in embryos. The 1,262-nt *mex-3* cDNA clone[20] was divided into two segments, *mex-3A* and *mex-3B*, with a short (325-nt) overlap (similar results were obtained in experiments with no overlap between interfering and probe segments). *mex-3B* antisense or dsRNA was injected into the gonads of adult animals, which were fed for 24 h before fixation and *in situ* hybridization (ref. 5; B. Harfe and A.F., unpublished observations). The *mex-3B* dsRNA produced 100% embryonic arrest, whereas >90% of embryos produced after the antisense injections hatched. Antisense probes for the *mex-3A* portion of *mex-3* were used to assay distribution of the endogenous *mex-3* mRNA (dark stain). four-cell-stage embryos are shown; similar results were observed from the one to eight cell stage and in the germ line of injected adults. **a**, Negative control showing lack of staining in the absence of the hybridization probe. **b**, Embryo from uninjected parent (showing normal pattern of endogenous *mex-3* RNA[20]). **c**, Embryo from a parent injected with purified *mex-3B* antisense RNA. These embryos (and the parent animals) retain the *mex-3* mRNA, although levels may be somewhat less than wild type. **d**, Embryo from a parent injected with dsRNA corresponding to *mex-3B*; no *mex-3* RNA is detected. Each embryo is approximately 50 μm in length.

Table 2 Effect of site of injection on interference in injected animals and their progeny

dsRNA	Site of injection	Injected-animal phenotype	Progeny phenotype
None	Gonad or body cavity	No twitching	No twitching
None	Gonad or body cavity	Strong nuclear and mitochondrial GFP expression	Strong nuclear and mitochondrial GFP expression
unc22B	Gonad	Weak twitchers	Strong twitchers
unc22B	Body-cavity head	Weak twitchers	Strong twitchers
unc22B	Body-cavity tail	Weak twitchers	Strong twitchers
gfpG	Gonad	Lower nuclear and mitochondiral GFP expression	Rare or absent nuclear and mitochondiral GFP expression
gfpG	Body-cavity tail	Lower nuclear and mitochondrial GFP expression	Rare or absent nuclear and mitochondrial GFP expression
lacZL	Gonad	Lower nuclear GFP expression	Rare or absent nuclear-GFP expression
lacZL	Body-cavity tail	Lower nuclear GFP expresison	Rare or absent nuclear-GFP expression

The GFP-reporter strain PD4251, which expresses both mitochondrial GFP and nuclear GFP–LacZ, was used for injections. The use of this strain allowed simultaneous assay for interference with *gfp* (fainter overall fluorescence), *lacZ* (loss of nuclear fluorescence) and *unc-22* (twitching). Body-cavity injections into the tail region were carried out to minimize accidental injection of the gonad; equivalent results have been observed with injections into the anterior body cavity. An equivalent set of injections was also performed into a single gonad arm. The entire progeny broods showed phenotypes identical to those described in Table 1. This included progeny of both injected and uninjected gonad arms. Injected animals were scored three days after recovery and showed somewhat less dramatic phenotypes than their progeny. This could be partly due to the persistence of products already present in the injected adult. After injection of double-stranded *unc22B*, a fraction of the injected animals twitch weakly under standard growth conditions (10 out of 21 animals). Levamisole treatment led to twitching of 100% (21 out of 21) of these animals. Similar effects (not shown) were seen with double-stranded *unc22A*. Injections of double-stranded *gfpG* or double-stranded *lacZL* produced a dramatic decrease (but not elimination) of the corresponding GFP reporters. In some cases, isolated cells or parts of animals retained strong GFP activity. These were most frequently seen in the anterior region and around the vulva. Injections of double-stranded *gfpG* and double-stranded *lacZL* produced no twitching, whereas injections of double-stranded *unc22A* produced no change in the GFP-fluorescence pattern.

in these injections. dsRNA injected into the body cavity or gonad of young adults also produced gene-specific interference in somatic tissues of the injected animal (Table 2).

The use of dsRNA injection adds to the tools available for studying gene function in *C. elegans*. In particular, it should now be possible functionally to analyse many interesting coding regions[21] for which no specific function has been defined. Although the effects of dsRNA-mediated interference are potent and specific we have observed several limitations that should be taken into account when designing RNA-interference-based experiments. First, a sequence shared between several closely related genes may interfere with several members of the gene family. Second, it is likely that a low level of expression will resist RNA-mediated interference for some or all genes, and that a small number of cells will likewise escape these effects.

Genetic tools are available for only a few organisms. Double-stranded RNA could conceivably mediate interference more generally in other nematodes, in other invertebrates, and, potentially, in vertebrates. RNA interference might also operate in plants: several studies have suggested that inverted-repeat structures or characteristics of dsRNA viruses are involved in transgene-dependent co-suppression in plants[22,23].

There are several possible mechanisms for RNA interference in *C. elegans*. A simple antisense model is not likely: annealing between a few injected RNA molecules and excess endogenous transcripts would not be expected to yield observable phenotypes. RNA-targeted processes cannot, however, be ruled out, as they could include a catalytic component. Alternatively, direct RNA-mediated interference at the level of chromatin structure or transcription could be involved. Interactions between RNA and the genome, combined with propagation of changes along chromatin, have been proposed in mammalian X-chromosome inactivation and plant-gene co-suppression[22,24]. If RNA interference in *C. elegans* works by such a mechanism, it would be new in targeting regions of the template that are present in the final mRNA (as we observed no phenotypic interference using intron or promoter sequences). Whatever their target, the mechanisms underlying RNA interference probably exist for a biological purpose. Genetic interference by dsRNA could be used by the organism for physiological gene silencing. Likewise, the ability of dsRNA to work at a distance from the site of injection, and particularly to move into both germline and muscle cells, suggests that there is an effective RNA-transport mechanism in *C. elegans*. □

Methods

RNA synthesis and microinjection. RNA was synthesized from phagemid clones by using T3 and T7 polymerase[6]. Templates were then removed with two sequential DNase treatments. When sense-, antisense-, and mixed-RNA populations were to be compared, RNAs were further purified by electrophoresis on low-gelling-temperature agarose. Gel-purified products appeared to lack many of the minor bands seen in the original 'sense' and 'antisense' preparations. Nonetheless, RNA species comprising <10% of purified RNA preparations would not have been observed. Without gel purification, the 'sense' and 'antisense' preparations produced notable interference. This interference activity was reduced or eliminated upon gel purification. In contrast, sense-plus-antisense mixtures of gel-purified and non-gel-purified RNA preparations produced identical effects.

Sense/antisense annealing was carried out in injection buffer (ref. 27) at 37 °C for 10–30 min. Formation of predominantly double-stranded material was confirmed by testing migration on a standard (nondenaturing) agarose gel: for each RNA pair, gel mobility was shifted to that expected for dsRNA of the appropriate length. Co-incubation of the two strands in a lower-salt buffer (5 mM Tris-Cl, pH 7.5, 0.5 mM EDTA) was insufficient for visible formation of dsRNA *in vitro*. Non-annealed sense-plus-antisense RNAs for *unc22B* and *gfpG* were tested for RNA interference and found to be much more active than the individual single strands, but twofold to fourfold less active than equivalent preannealed preparations.

After preannealing of the single strands for *unc22A*, the single electrophoretic species, corresponding in size to that expected for the dsRNA, was purified using two rounds of gel electrophoresis. This material retained a high degree of interference activity.

Except where noted, injection mixes were constructed so that animals would receive an average of 0.5×10^6 to 1.0×10^6 RNA molecules. For comparisons of sense, antisense, and double-stranded RNA activity, equal masses of RNA were injected (that is, dsRNA was used at half the molar concentration of the single strands). Numbers of molecules injected per adult are approximate and based on the concentration of RNA in the injected material (estimated from ethidium bromide staining) and the volume of injected material (estimated from visible displacement at the site of injection). It is likely that this volume will vary several-fold between individual animals; this variability would not affect any of the conclusions drawn from this work.

Analysis of phenotypes. Interference with endogenous genes was generally assayed in a wild-type genetic background (N2). Features analysed included movement, feeding, hatching, body shape, sexual identity, and fertility. Interference with *gfp* (ref. 25) and *lacZ* activity was assessed using *C. elegans* strain PD4251. This strain is a stable transgenic strain containing an integrated array (ccIs4251) made up of three plasmids: pSAK4 (*myo-3* promoter driving mitochondrially targeted GFP); pSAK2 (*myo-3* promoter driving a nuclear-targeted GFP–LacZ fusion); and a *dpy-20* subclone[26] as a selectable marker. This strain produces GFP in all body muscles, with a combination of mitochondrial and nuclear localization. The two distinct compartments are easily distinguished in these cells, allowing easy distinction between cells expressing both, either, or neither of the original GFP constructs.

Gonadal injection was done as described[27]. Body-cavity injections followed a similar procedure, with needle insertion into regions of the head and tail beyond the positions of the two gonad arms. Injection into the cytoplasm of intestinal cells is also effective, and may be the least disruptive to the animal. After recovery and transfer to standard solid media, injected animals were transferred to fresh culture plates at 16-h intervals. This yields a series of semisynchronous cohorts in which it was straightforward to identify phenotypic differences. A characteristic temporal pattern of phenotypic severity is observed among progeny. First, there is a short 'clearance' interval in which unaffected progeny are produced. These include impermeable fertilized eggs present at the time of injection. Second, after the clearance period, individuals that show the interference phenotype are produced. Third, after injected animals have produced eggs for several days, gonads can in some cases 'revert' to produce incompletely affected or phenotypically normal progeny.

Received 16 September; accepted 24 November 1997.

1. Izant, J. & Weintraub, H. Inhibition of thymidine kinase gene expression by antisense RNA: a molecular approach to genetic analysis. *Cell* **36,** 1007–1015 (1984).
2. Nellen, W. & Lichtenstein, C. What makes an mRNA anti-sense-itive? *Trends Biochem. Sci.* **18,** 419–423 (1993).
3. Fire, A., Albertson, D., Harrison, S. & Moerman, D. Production of antisense RNA leads to effective and specific inhibition of gene expression in *C. elegans* muscle. *Development* **113,** 503–514 (1991).
4. Guo, S. & Kemphues, K. *par-1*, a gene required for establishing polarity in *C. elegans* embryos, encodes a putative Ser/Thr kinase that is asymmetrically distributed. *Cell* **81,** 611–620 (1995).
5. Seydoux, G. & Fire, A. Soma-germline asymmetry in the distributions of embryonic RNAs in *Caenorhabditis elegans*. *Development* **120,** 2823–2834 (1994).
6. Ausubel, F. *et al. Current Protocols in Molecular Biology* (Wiley, New York, 1990).
7. Brenner, S. The genetics of *Caenorhabditis elegans*. *Genetics* **77,** 71–94 (1974).
8. Moerman, D. & Baillie, D. Genetic organization in *Caenorhabditis elegans*: fine structure analysis of the *unc-22* gene. *Genetics* **91,** 95–104 (1979).
9. Benian, G., L'Hernault, S. & Morris, M. Additional sequence complexity in the muscle gene, *unc-22*, and its encoded protein, twitchin, of *Caenorhabiditis elegans*. *Genetics* **134,** 1097–1104 (1993).
10. Proud, C. PKR: a new name and new roles. *Trends Biochem. Sci.* **20,** 241–246 (1995).
11. Epstein, H., Waterston, R. & Brenner, S. A mutant affecting the heavy chain of myosin in *C. elegans*. *J. Mol. Biol.* **90,** 291–300 (1974).
12. Karn, J., Brenner, S. & Barnett, L. Protein structural domains in the *C. elegans unc-54* myosin heavy chain gene are not separated by introns. *Proc. Natl Acad. Sci. USA* **80,** 4253–4257 (1983).
13. Doniach, T. & Hodgkin, J. A. A sex-determining gene, *fem-1*, required for both male and hermaphrodite development in *C. elegans*. *Dev. Biol.* **106,** 223–235 (1984).
14. Spence, A., Coulson, A. & Hodgkin, J. The product of *fem-1*, a nematode sex-determining gene, contains a motif found in cell cycle control proteins and receptors for cell–cell interactions. *Cell* **60,** 981–990 (1990).
15. Krause, M., Fire, A., Harrison, S., Priess, J. & Weintraub, H. CeMyoD accumulation defines the body wall muscle cell fate during *C. elegans* embryogenesis. *Cell* **63,** 907–919 (1990).
16. Chen, L., Krause, M., Sepanski, M. & Fire, A. The *C. elegans* MyoD homolog *HLH-1* is essential for proper muscle function and complete morphogenesis. *Development* **120,** 1631–1641 (1994).
17. Dibb, N. J., Maruyama, I. N., Krause, M. (**Author: OK?**) & Karn, J. Sequence analysis of the complete *Caenorhabditis elegans* myosin heavy chain gene family. *J. Mol. Biol.* **205,** 603–613 (1989).
18. Sulston, J., Schierenberg, E., White, J. & Thomson, J. The embryonic cell lineage of the nematode *Caenorhabditis elegans*. *Dev. Biol.* **100,** 64–119 (1983).
19. Sulston, J. & Horvitz, H. Postembyonic cell lineages of the nematode *Caenorhabiditis elegans*. *Dev. Biol.* **82,** 41–55 (1977).

20. Draper, B. W., Mello, C. C., Bowerman, B., Hardin, J. & Priess, J. R. *MEX-3* is a KH domain protein that regulates blastomere identity in early *C. elegans* embryos. *Cell* **87,** 205–216 (1996).
21. Sulston, J. *et al.* The *C. elegans* genome sequencing project: a beginning. *Nature* **356,** 37–41 (1992).
22. Matzke, M. & Matzke, A. How and why do plants inactivate homologous (*trans*) genes? *Plant Physiol.* **107,** 679–685 (1995).
23. Ratcliff, F., Harrison, B. & Baulcombe, D. A similarity between viral defense and gene silencing in plants. *Science* **276,** 1558–1560 (1997).
24. Latham, K. X chromosome imprinting and inactivation in the early mammalian embryo. *Trends Genet.* **12,** 134–138 (1996).
25. Chalfie, M., Tu, Y., Euskirchen, G., Ward, W. & Prasher, D. Green fluorescent protein as a marker for gene expression. *Science* **263,** 802–805 (1994).
26. Clark, D., Suleman, D., Beckenbach, K., Gilchrist, E. & Baillie, D. Molecular cloning and characterization of the *dpy-20* gene of *C. elegans*. *Mol. Gen. Genet.* **247,** 367–378 (1995).
27. Mello, C. & Fire, A. DNA transformation. *Methods Cell Biol.* **48,** 451–482 (1995).

Supplementary information is available on *Nature*'s World-Wide Web site (http://www.nature.com) or as paper copy from Mary Sheehan at the London editorial office of *Nature*.

Acknowledgements. We thank A. Grishok, B. Harfe, M. Hsu, B. Kelly, J. Hsieh, M. Krause, M. Park, W. Sharrock, T. Shin, M. Soto and H. Tabara for discussion. This work was supported by the NIGMS (A.F.) and the NICHD (C.M.), and by fellowship and career awards from the NICHD (M.K.M.), NIGMS (S.K.), PEW charitable trust (C.M.), American Cancer Society (C.M.), and March of Dimes (C.M.).

Correspondence and requests for materials should be addressed to A.F. (e-mail: fire@mail1.ciwemb.edu).

Role of the histone deacetylase complex in acute promyelocytic leukaemia

Richard J. Lin*†‡, Laszlo Nagy*†, Satoshi Inoue†, Wenlin Shao§, Wilson H. Miller Jr§ & Ronald M. Evans*†

** Howard Hughes Medical Institute, and †The Salk Institute for Biological Studies, La Jolla, California 92037, USA*
‡ Graduate Program in Molecular Pathology, University of California San Diego, School of Medicine, La Jolla, California 92093, USA
§ Lady Davis Institute for Medical Research, McGill University Departments of Oncology and Medicine, Montreal, Quebec, Canada H3T 1E2

Non-liganded retinoic acid receptors (RARs) repress transcription of target genes by recruiting the histone deacetylase complex[1–3] through a class of silencing mediators termed SMRT or N-CoR[4,5]. Mutant forms of RARα, created by chromosomal translocations with either the PML (for promyelocytic leukaemia)[6–8] or the PLZF (for promyelocytic leukaemia zinc finger)[9,10] locus, are oncogenic and result in human acute promyelocytic leukaemia (APL). PML–RARα APL patients achieve complete remission following treatments with pharmacological doses of retinoic acids (RA); in contrast, PLZF–RARα patients respond very poorly, if at all[11]. Here we report that the association of these two chimaeric receptors with the histone deacetylase (HDAC) complex helps to determine both the development of APL and the ability of patients to respond to retinoids. Consistent with these observations, inhibitors of histone deacetylase dramatically potentiate retinoid-induced differentiation of RA-sensitive, and restore retinoid responses of RA-resistant, APL cell lines. Our findings suggest that oncogenic RARs mediate leukaemogenesis through aberrant chromatin acetylation, and that pharmacological manipulation of nuclear receptor co-factors may be a useful approach in the treatment of human disease.

Because both PML–RARα and PLZF–RARα inhibit normal retinoid signalling[6–14], we reasoned that identification of factors associated with these proteins might provide mechanistic insights into their oncogenic functions. PLZF–RARα retains the autonomous repression domain, the BTB/POZ (for bric-à-brac/tramtrack/broad complex, poxvirus and zinc-finger) domain, from PLZF[15]. Because deletion of this domain abolishes the biological functions of PLZF–RARα *in vivo*[16,17], we investigated whether it might associate directly with components of the nuclear receptor co-repressor complex[1–3]. By using an *in vitro* interaction assay, we found that radiolabelled full-length mSin3A and histone deacetylase 1 (HDAC1), but not mSin3B, were specifically retained on matrix-bound fusion proteins of glutathione *S*-transferase with the BTB/POZ domain of PLZF (GST–PLZF; Fig. 1a). Results from a yeast two-hybrid assay showed that PLZF interacts with all known components of the co-repressor complex *in vivo* (Fig. 1b). We further mapped the PLZF interaction domain in mSin3A to the paired amphipathic helix 1 (PAH1, residues 112–192) by a mammalian two-hybrid assay (Fig. 1c). Finally, using a co-immunoprecipitation assay from nuclear extracts of transfected CV1 cells, we confirmed that PLZF, SMRT, mSin3A and HDAC1 form a complex in mammalian cells (Fig. 1d). These results, together with the finding that SMRT interacts with another BTB/POZ oncoprotein, LAZ3/BCL6 (ref. 18), demonstrated that this family of transcriptional factors recruits histone deacetylases to repress transcription and implicates histone deacetylases in cellular transformation.

By using a yeast two-hybrid assay, we demonstrated that PLZF–RARα interacts directly with both SMRT and mSin3A, whereas PML–RARα interacts only with SMRT[19] (Fig. 2B). Most importantly, we showed using a co-immunoprecipitation assay that HDAC1 exists in a complex with either PLZF–RARα or PML–RARα in transfected CV1 cells (Fig. 2C). Furthermore, a similar assay using nuclear extracts of the NB4 cells established from a patient with t(15:17) APL[20] indicated that endogenous HDAC1 can be co-precipitated with an anti-PML antibody (Fig. 2D). The presence of endogenous PML–RARα was confirmed by immunoblotting analyses using anti-PML and anti-RARα antibodies (data

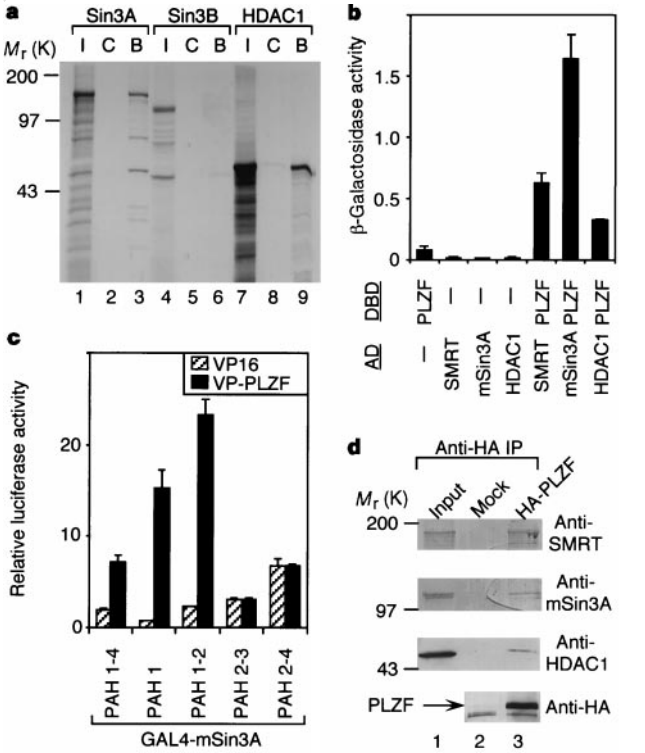

Figure 1 Association of co-repressors and HDAC1 with PLZF. **a**, SDS–PAGE analysis of ^{35}S-labelled mSin3A, mSin3B or HDAC1 proteins retained on immobilized GST–PLZF affinity matrices. I, 20% input; C, GST control; B, bound. **b**, Interactions between PLZF and full-length SMRT, mSin3A or HDAC1 in a yeast two-hybrid assay. **c**, Interactions between GAL4–DBD fusions of different PAHs of mSin3A and VP16 fusion of PLZF are analysed by a mammalian two-hybrid assay in CV1 cells. **d**, PLZF associates with the histone deacetylase complex *in vivo*. CV1 cells were transfected with either vectors only (mock) or plasmids encoding HA–PLZF, SMRT, mSin3A and HDAC1 (HA–PLZF) and nuclear extracts were immunoprecipitated (IP) using anti-HA antibodies followed by immunoblotting analyses using antibodies against SMRT, mSin3A and HDAC1. In lane 1, ~100 μg of nuclear extract was applied to ascertain the positions of blotted proteins (input).